Characterization of anti-GASP motif antibodies that inhibit the interaction between GPRASP1 and G protein-coupled receptors

Gabrielle Zeder Lutz, Olivier Bornert, Rosine Fellmann-Clauss, Adeline Knittel-Obrecht, Thibaud Tranchant, Sarah Bouteben, Juliette Kaeffer, Raphaëlle Quillet, Pascal Villa, Renaud Wagner, et al.

Characterization of anti-GASP motif antibodies that inhibit the interaction between GPRASP1 and G protein-coupled receptors

Gabrielle Zeder-Lutz[a], Olivier Bornert[a], Rosine Fellmann-Clauss[a], Adeline Knittel-Obrecht[b], Thibaud Tranchant[a], Sarah Bouteben[a,c], Juliette Kaeffer[a], Raphaëlle Quillet[a,], Pascal Villa[b], Renaud Wagner[a,c], Sandra Lecat[a*] and Frédéric Simonin[a*]

Affiliations:

[a] Biotechnology and Cell Signaling, UMR7242 CNRS, University of Strasbourg, Illkirch-Graffenstaden, France.

[b] Plateforme de chimie biologique integrative de Strasbourg, UAR3286, CNRS, University of Strasbourg, Illkirch-Graffenstaden, France.

[c] Biotechnology and Cell Signaling, IMPReSs facility for Integral Membrane Proteins Research and Services, UMR7242 CNRS, University of Strasbourg, Illkirch-Graffenstaden, France

* Co-last authors

Corresponding author:

Dr. Frédéric Simonin, Biotechnology and Cell Signaling, UMR7242 CNRS, University of Strasbourg, 300 Boulevard Sébastien Brant, 67412, Illkirch, France. E-mail address: simonin@unistra.fr

ABSTRACT

G protein-coupled receptor associated sorting protein 1 (GPRASP1) belongs to a family of 10 proteins that display sequence homologies in their C-terminal region. Several members including GPRASP1 also display a short repeated sequence called the GASP motif that is critically involved in protein-protein interactions with G protein-coupled receptors (GPCRs). Here, we characterized anti-GASP motif antibodies and investigated their potential inhibitory functions. We first showed that our in-house anti-GPRASP1 rabbit polyclonal serum contains anti-GASP motif antibodies and purified them by affinity chromatography. We further showed that these antibodies can detect GPRASP1 and GPRASP2 in Western blot, immunoprecipitation and immunofluorescence experiments while a mutant of GPRASP2, in which the most conserved hydrophobic core of the GASP motifs is mutated, was no more detected. Further characterization of anti-GASP motif antibodies by ELISA and Surface Plasmon Resonance assays suggests that GASP motifs function as multivalent epitopes. Finally, we set-up an Amplified Luminescent Proximity Homogeneous AlphaScreen® assay to detect the interaction between purified ADRB2 receptor and the central domain of GPRASP1 and showed that anti-GASP motif antibodies efficiently inhibit this interaction. Altogether, our results suggest that anti-GASP motif antibodies could represent a valuable tool to neutralize the interaction of GPRASP1 and GPRASP2 with different GPCRs.

Keywords: Intrinsically disordered regions, PPI, GASP motif, GPRASP1 antibodies, SPR, AlphaScreen assay

1. Introduction

The GPRASP/ARMCX protein family, mainly present in mammals, is composed of ten members, nine of which are encoded in tandem on the X chromosome. They share homologies in their carboxyl-terminal domains that contain armadillo-like repeats and can be subdivided according to whether they possess or not GASP motif repeats (subfamily 1 and 2, respectively; Abu-Helo and Simonin, 2010; Bornert et al., 2013; Kaeffer et al., 2021; Simonin et al., 2004). GPRASP1 and GPRASP2 (GPCR-associated sorting proteins) are the best functionally characterized proteins of subfamily 1 and have been implicated in membrane trafficking of G protein-coupled receptors (GPCRs; Jung et al., 2016; Kaeffer et al., 2021; Morales-Hernandez et al., 2020; Whistler et al., 2002). However, the molecular functions of GPRASP1 and GPRASP2 remain to be precisely characterized and knowledge about their intracellular localization and regulation is missing.

In previous studies, we have identified and characterized the GASP motif as a consensus sequence of twenty-one residues, the fifteen most conserved residues being formed by a hydrophobic kernel tetrapeptide - serine-tryptophan-phenylalanine-tryptophan (SWFW) - surrounded by acidic amino acids (Kaeffer et al., 2021). The GASP motif repeats are located in the central part of the proteins, which is considered an intrinsically disordered region, and are unique to the GPRASP/ARMCX subfamily 1 of all proteins in the Swissprot database (Simonin et al., 2004; Kaeffer et al., 2021). In Human, GASP motifs are found in tandems, 22 times in GPRASP1, 7 times in GPRASP2, 2.5 times in GPRASP3, 11 times in ARMCX4 and 1.5 times in ARMCX5 (Kaeffer et al., 2021). We have shown previously that GASP motifs are necessary for GPRASP1 or GPRASP2 to interact directly with several GPCRs (Bornert et al., 2013). We have observed that *in vitro* translated full-length GPRASP1 could be pulled-down by the purified GST-tagged C-tail of GPCRs including delta-opioid, muscarinic M1 and beta-adrenergic ADRB1 receptors. Moreover, the central domain of GPRASP1 on its own could be pulled-down to the same extent by these receptor C-tails. Since this central domain contains 19 GASP motifs, this motif may play a major role in mediating these interactions. In cells, exogenously expressed full-length muscarinic M1 receptor, beta-adrenergic ADRB1 or ADRB2 receptors and calcitonin-like CALCR, could all co-immunoprecipitate the full-length GPRASP1 as well as the central domain of GPRASP1 expressed on its own. Using Surface Plasmon Resonance (SPR) measurements, we have shown that the purified central domain of GPRASP1 could

interact in *vitro* with purified full-length ADRB2 or cannabinoid type 2 CNR2 receptors with an apparent affinity of 10 to 100nM (Bornert et al., 2013). Interestingly, GST-pull-down experiments or SPR measurements allowed us to show that the interaction between these receptors and full-length GPRASP1 or the central domain of GPRASP1 (respectively) is completely abolished by a small peptide encoding one of the GASP motifs of GPRASP2 used as a competitor (Bornert et al., 2013). Finally, GPRASP2 can be pulled-down by purified GST-tagged C-tail of several GPCRs while a mutant of GPRASP2 in which the consensus kernel SWFW of GASP motifs was substituted by four alanine residues is no longer pulled-down (Bornert et al., 2013). These results indicate that GASP motifs mediate protein/protein interactions in particular with GPCRs.

We have previously generated and validated in GPRASP1 knock-out mice a rabbit polyclonal serum directed against GPRASP1 (Boeuf et al., 2009). To generate antibodies, one approach consists in producing a short peptide of 10 to 20 amino acids that is predicted to represent an immunogenic region of the targeted protein. A drawback of this approach is that many anti-peptide antibodies can react with the peptide but fail to recognize the cognate protein. Another approach is to produce the target protein as the immunogen for inoculation into animals, which, as a general rule, produces antibodies that can recognize the native protein and often display interfering function. We employed this latter to generate rabbit polyclonal anti-GPRASP1 antibodies directed against the last 470 residues of the GPRASP1. This region of GPRASP1 corresponds to the sequence initially isolated as a prey from a two-hybrid screen using the C-tail of delta-opioid receptor as a bait (Simonin et al., 2004). To raise antibodies, we produced and purified from E Coli GST fused to $GPRASP_{924-1395}$ and injected it to two rabbits. Within this immunogenic sequence, the majority codes for the most conserved C-ter domain of the GPRASP/ARMCX protein family with armadillo-like repeats but it extends on its N-terminus to include three GASP motifs repeated in tandem. We have previously observed that the resulting polyclonal serum could label the central domain of GPRASP1 (Bornert et al., 2013) suggesting that it might contain anti-GASP motif antibodies. In the present study, we have purified from this serum and further characterized subpopulations of antibodies that specifically recognize GASP motifs. Using these anti-GASP motif antibodies, we have set-up and validated a miniaturized assay suitable for the identification of compounds that inhibit the ADRB2 receptor/GPRASP1 interaction.

2. Experimental Section

2.1 Cloning of GPRASP/ARMCX coding sequences into mammalian and bacterial expression vectors

All the constructs that were used in this study are summarized in Table 1. The cDNAs encoding the full-length proteins GPRASP1, GPRASP2, GPRASP2-DM, GPRASP3 and ARMCX5 cloned into the pcDNA3 or pcDNA3.1 eukaryotic expression vectors were described elsewhere (Bornert et al., 2013; Simonin et al., 2004). For the expression of the EYFP-GPRASP1 and EYFP-GPRASP2 fusion proteins, the sequence encoding the enhanced yellow fluorescent protein (EYFP, Clontech) was fused 5' upstream to each of these cDNA and inserted into the pcDNA3.1/Hygromycin (+) vector. For the expression of each GPRASP/ARMCX proteins fused at the C-ter of the *Gaussia princeps* luciferase GLuc2 fragment according to (Poirson et al., 2017), PCR fragments were cloned into pDONOR223 (GPRASP1 and GPRASP2) or pDONOR207 (GPRASP3 and ARMCX5) following the Gateway cloning scheme and then subcloned by LR recombination into pSPICA-N2 vector (derived from the pCiNeo mammalian expression vector). The cDNAs encoding the different domains of GPRASP1 or GPRASP2 in fusion at their N-terminus with different proteins or tags were cloned into different vectors for *E. coli* expression: pGEX-4T3 vectors for bacterial expression of GST (glutathione S-transferase)-fused to sequences encoding full-length GPRASP1, the original antigen (o.Ag) encompassing residues 924 to 1395 of GPRASP1 and GPRASP2-C encompassing residues 367 to 838 of GPRASP2. The Middle domain of GPRASP1, GPRASP1-M, encoding residues 380 to 1073 was also cloned into pGEX-4T3 (Bornert et al., 2013; Simonin et al., 2004). pMALC2x vector was used for bacterial expression of the MBP (maltose binding protein) fused GPRASP1 protein domains: the o.Ag, the GPRASP1-Ct encompassing residues 1147 to 1395 and the GPRASP1-M. pET28b vector was used for bacterial expression of the GASP peptide encoding residues 800 to 889 of GPRASP1 fused to a hexa-Histidine-tag (6xHis). All constructs were verified by DNA sequencing.

2.2. Expression and Purification of GPRASP1 Fusion Proteins (Table 1)

GST-GPRASP1 full-length protein was expressed and purified as previously described (Bornert et al., 2013). To express the 6xHis-GASP peptide and the recombinant MBP proteins, vectors were introduced into competent *E. coli* Rosetta 2 DE3 strain (NOVAGEN 71400) and expression was induced using 0.5 mM

isopropylthiogalactoside (IPTG) for 18 h at 22 °C (MBP-GPRASP1-M) or 1 mM IPTG for 2,5 h at 37 °C (6xHis-GASP peptide; MBP-o.Ag, MBP-GPRASP1-Ct). Bacteria were then pelleted, suspended in ice-cold lysis buffer (20 mM Tris pH 7.5; 200 mM NaCl; 1 mM DTT with cOmplete protease inhibitors cocktail (ROCHE)), lysed using the microfluidizer M110-EH-30 or a sonicator (40W). Finally, the lysates were cleared by centrifugation (10,000 g, 15 min, 4 °C). The MBP alone and MBP-fused GPRASP1 domains were purified on an AKTA Purifier instrument (GE Healthcare) using an MBP-Trap 1 ml column (Cytiva Europe GmbH) according to the manufacturer instructions. Proteins were eluted with lysis buffer supplemented with 10 mM maltose. The fractions corresponding to the protein of interest were pooled and concentrated using Vivaspin6 centrifugal concentrator with a 50 kDa cut-off (Sartorius) and dialyzed to exchange the buffer for PBS or for the coupling buffer (0.2 M NaHCO3 pH 8.3; 0.5 M NaCl) when used to prepare columns for anti-GST-o.Ag serum affinity purification. All fusion proteins with purified GPRASP1 domains were quantified using the BCA assay (Pierce), analyzed by SDS-PAGE and stored at -20 °C.

2.3. Affinity Purification of antibodies sub-populations from serum against GST-o.Ag protein

Different purified MBP-fused GPRASP1 domains were immobilized onto affinity columns in order to purify antigen-specific antibodies from the serum with polyclonal rabbit antibodies directed against the GST-o.Ag fusion protein (Simonin et al., 2004). The purified MBP-fused GPRASP1 domains were cross-linked via amine groups onto the pre-packed NHS-activated Sepharose™ columns (HiTrap NHS-activated HP; Cytiva Europe GmbH) according to the instructions from the manufacturer and equilibrated in PBS before their further use. To purify antibodies, total IgGs fraction was first prepared from 1 to 2 ml of serum diluted 2-fold with binding buffer (PBS) using a HiTrap Protein A HP 1 ml column (Cytiva Europe GmbH). The IgGs were eluted with 200 mM citric acid, pH 2.5 (elution buffer) into neutralizing buffer (1 M Tris-HCl, pH 8) and dialyzed against PBS before their adsorption by recirculation onto MBP-GPRASP1 domain-affinity columns. After incubation for 4 h to 12 h at 4 °C, each affinity column was washed with 10 ml PBS. Antibodies were eluted with 0.5 ml elution buffer into 1.5 ml tubes pre-loaded with 0.05 ml neutralizing buffer.

2.4 Cell Culture and Transfection

Cells were grown at 37 °C in a water-saturated atmosphere containing 5 % CO2 incubator. HEK293 cells lines (Vollmer et al., 1999) were grown in Dulbecco's Modified Eagle's Medium (DMEM, Gibco) with 4.5 g/l glucose, 4 mM L-glutamine, 1 mM sodium pyruvate, and 10 % (v/v) fetal bovine serum (Gibco), penicillin and streptomycin (100 U/ml and 100 µg/ml) antibiotics. For transient transfection, cells were seeded at 5 to 6.10^5 cells/well in 6-wells culture plates. 24 h after seeding (80 % confluency) DNA transfection was started by adding 4 µg of plasmid DNA and 9 µg of PEImax reagent (24765-1, Polysciences; Europe). Cell lysates were prepared 24 h later in ice-cold RIPA buffer (50 mM Tris-HCl pH 7.4; 150 mM NaCl; 1 % (v/v) NP40; 0.25 % (w/v) Na-deoxycholate) supplemented with EDTA-free anti-protease and protein concentrations were determined (BCA assay kit, Pierce). Chinese hamster ovary (CHO) cells were maintained in Dulbecco's modified Eagle's medium supplemented with HAMF12 (DMEM/HAMF12 1:1, Gibco) containing 5 % (v/v) fetal calf serum (Gibco), penicillin and streptomycin antibiotics (100 U/ml and 100 µg/ml, respectively) and 2 mM L-glutamine. CHO cells stably expressing either EYFP-GPRASP1 or EYFP-GPRASP2 after lipofectamine 2000 transfection were established with the help of FACS sorting and propagated in appropriate selection media supplemented with 0.4 mg/ml Hygromycin. Human SH-SY5Y neuroblastoma cells were grown in RPMI medium, 4 mM L-glutamine, and 10% (v/v) fetal bovine serum (Gibco), penicillin and streptomycin antibiotics (100 U/ml and 100 µg/ml, respectively).

2.5. Generation of GPRASP2-KO HEK293 cell line by CRISPR/Cas9 technology

HEK293 cells were genome edited using clustered regularly interspaced short palindromic repeats (CRISPR)/CRISPR-associated 9 (Cas9) system. To ensure the high specificity to the target sites, three different selective GPRASP2 guided-RNAs (gRNA 1, 2 and 3) were tested using web-based algorithms (https://www.dna20.com/eCommerce/cas9/input) and verified on NCBI blast. The gRNAs were also controlled for genome-wide off-target analysis using CCTop, (http://crispr.cos.uni-heidelberg (Stemmer et al., 2015). gRNA 1, 2 and 3 had the following sequences: gRNA1, 5'-CACCGCTGGGGAAGAGGTTATCGC; gRNA2, 5'-CACCGTTAGGACCCAGGCAACTAC and gRNA3, 5'-CACCGGAGACCAAGTCTGTGCCTG. Each gRNA was subcloned into pSpCas9(BB)-2A-GFP (PX458) (Addgene plasmid # 48138, gift from Feng Zhang). Forty-eight hours after cell transfection with 166.7 ng plasmid/cm² using the calcium

phosphate technique (Kingston et al., 2003), GFP positive cells were sorted by flow cytometry (FACS Aria, Becton Dickinson) and were allowed to grow prior to GPRASP2 expression analysis by Western blotting using anti-GST-o.Ag serum. The promising polyclonal cell populations in term of large decrease of GPRASP2 expression were diluted in order to collect clones after 3 weeks of growth in T10 plates. GPRASP2-KO HEK293 clones could be obtained with the three gRNAs. GPRASP2-KO HEK293 clone N°2 generated using gRNA2 was further used in this study.

2.6 Mouse brain total homogenates preparation

Brain tissue samples of WT and GPRASP1 deficient mice (Boeuf et al., 2009) were homogenized with an UltraTurrax device (IKA) followed by several dounce passages (IMLAB) in a final volume of 20 ml/g of tissue of 50 mM Tris-HCl, pH 7.4, 1 mM EDTA, 250 mM Sucrose, and the homogenate was centrifuged for 10 min at 500 g at 4 °C. The supernatant was then collected and protein concentrations were determined by BCA assay kit (Pierce).

2.7 Immunoprecipitation experiments

CHO cells stably expressing N-terminally EYFP-tagged GPRASP1 or GPRASP2 grown in petri dishes were washed twice with PBS and lysed in a buffer containing 10 mM Tris-HCl, pH 7.4, 150 mM NaCl, 25 mM KCl, 0.3 % (v/v) Triton X-100 and cOmplete protease inhibitors (Roche) for 1 h at 4 °C under agitation. 250 µg of proteins from the cleared lysates were incubated with 1.5 µg (20nM) of the indicated affinity-purified anti-GPRASP1 population overnight at 4 °C, followed by an incubation with 50 µl of protein A MAG-Sepharose (GE Healthcare) for an additional 3 h at 4 °C. Beads were then washed three times in ice-cold lysis buffer.

2.8 SDS-PAGE and Immunoblotting

HEK293 cells lysates, brain homogenates or immuno-precipitates were mixed in Laemmli buffer and incubated at 100 °C for 5 min. Proteins were separated by electrophoresis on SDS 8 % polyacrylamide gels and transferred to PVDF membranes (IMMOBILON P, Merck). After 1 h incubation with blocking buffer (3 % (w/v) BSA in PBS + 0.04 % (v/v) Tween-20 (PBST)) at room temperature (RT), membranes were incubated with primary antibodies overnight at 4 °C. Membranes were washed 3 times with PBST (5 min/each) and incubated for 1 h at RT with Goat anti-rabbit horseradish peroxidase (HRP)-conjugated secondary antibody (1:50000) (Jackson ImmunoResearch). Blots were washed five times (5 min each) with PBST, prior to

imaging. Blots were developed using enhanced chemiluminescence (West Pico Plus, PIERCE) and the Amersham Imager 680 system (Cytiva Europe GmbH). Antibodies used were rabbit anti-Gaussia luciferase (NEB, E8023S) (Poirson et al., 2017) and anti-GFP-HRP (Ab6663 Goat polyclonal to GFP, Abcam).

2.9 ELISA and SPR Measurements

For the ELISA assays, microtiter wells (Nunc MaxiSorp™ThermoFisher Scientific) were coated either with purified MBP-o.Ag (1 nM), MBP-GPRASP1-M (1 nM) or MBP-GPRASP1-Ct (10 nM) in PBS over-night at 4 °C. After a saturation step (3 % (w/v) BSA in PBST) of 1 h at RT, the indicated purified polyclonal antibodies subpopulation was diluted in PBST and incubated at RT for 2 h. After three washes with PBST, antigen-antibodies complexes were revealed with addition of HRP-conjugated goat anti-rabbit IgG (Jackson ImmunoResearch). After several washes with PBST and addition of 3′,3′,5′,5′-tetramethylbenizidine (Sigma-Aldrich) in Citrate-Phosphate buffer 0.1 M pH 5, the optical density was measured at 450 nm in an ELISA reader.

The SPR measurements were achieved with a Biacore 2000 SPR instrument (GE Healthcare) equipped with a Sensor Chip CM5 (GE Healthcare) at 25 °C with HBS-EP (GE Healthcare) as the running buffer. The SPR signal (in ‘resonance units’; RU) was monitored in real time and shown as sensorgrams (RU vs time plots). According to (Stenberg et al., 1991), an SPR signal of 1000 RU corresponds to 1 ng⁄mm² of immobilized protein). Affinity-purified polyclonal anti-GST antibodies (GE Healthcare) were covalently immobilized in 4 flow cells using Amine Coupling Kit (GE Healthcare) according to the instructions from the manufacturer. Recombinant GST alone or indicated GST-fused GPRASP1 or GPRASP2 domains were captured and the GST surface was used as reference. Two concentrations of the indicated affinity-purified anti-GPRASP1 antibodies subpopulations were passed over GST (reference cell, 854 RU ~28,5 fmol/mm²); GST-GPRASP1 full-length (700 RU ~4.1 fmol/mm²) GST-GPRASP1-M (1160 RU ~10.5 4.1 fmol/mm²) and GST-GPRASP2-C (1393 RU ~ 18.6 fmol/mm²). Signals were corrected for signals from the reference flow cell and were normalized relative to target density as RU / fmol.mm².

2.10 Immunofluorescence microscopy

About 5 to 6.10^5 cells were seeded on fibronectin-coated 18 mm glass coverslip in 6 wells plates. After 24 hours (80 % confluency), cells were transfected with the

corresponding expression vectors using Lipofectamine2000, according to the manufacturer instructions. For the analysis by immunofluorescence microscopy, cells were fixed with 4 % (v/v) paraformaldehyde (Electron Microscopy Sciences, Euromedex) in PBS for 10 min and permeabilized with PBS + 0.1 % (v/v) Triton X100 for 10 min. After a blocking step (3 % (w/v) BSA in PBS, 60 min) fixed cells were incubated with the indicated affinity-purified anti-GPRASP antibodies subpopulations diluted in PBS over night at 4 °C. The bound antibodies were detected with Alexa Fluor 594 labeled-goat anti-rabbit immunoglobulins incubated during 60 min (Molecular probes). Nuclei were stained with 4′,6′-diamino-2phenyl-indole (DAPI 1 µg/ml, 5 mn). After several washes with PBS, the coverslips were mounted with Mowiol (CALBIOCHEM) and imaged with a microscope (DM5500 Leica) equipped with a 63X objective. The signal was recorded with a DFC350FX R2 camera (Leica). Confocal microscopy was performed with DMI 4000 (Leica). All microscopy images were processed using the Fiji/Image J software. The YFP detection in immunofluorescence experiments with the CHO cells stabilized for EYFP-GPRASP1 or EYFP-GPRASP2 expression was performed with a mouse monoclonal anti-GFP antibody (Life technologies A11120, 0.5 µg/ml, overnight at 4 °C) and YFP-mab complexes were revealed with an Alexa Fluor488 labeled-goat anti-mouse immunoglobulins 4 µg/ml, overnight at 4 °C (Molecular probes).

2.11 AlphaScreen experiments

Cross-titration of His-tagged ADRB2 receptor (2000-125 nM) against GST-GPRASP1-M (250-62.5 nM) was performed in 384 well plates (Optiplate, Perkin-Elmer, USA). Resulting combinations were mixed and incubated for 60 minutes at 25 °C. Glutathione Donor Beads (Perkin-Elmer) and Nickel Chelate Acceptor Beads (AlphaScreen Histidine Detection Kit; Perkin-Elmer) were then added to a final concentration of 20 µg/ml, incubated for 60 min and plates were then read using an EnVision Plate Reader (Perkin-Elmer). For the antibody competition assay, solubilized and purified His-tagged ADRB2 receptor (described in Bornert et al., 2013) and purified GST-GPRASP1-M were diluted in PBS at pH 7.0, 0.1 % (w/v) BSA, and 0.1 % (v/v) Tween20. The ADRB2 receptor (125 nM) was incubated with the GST-GPRASP1-M (62.5 nM) preincubated for 60 min at RT in presence of purified antibodies (concentration range of 0-800 nM) in 384-well plates (Optiplate, Perkin-Elmer). Glutathione Donor Beads Perkin-Elmer) and Nickel Chelate Acceptor Beads

(AlphaScreen Histidine Detection Kit, Perkin-Elmer) were then added to a final concentration of 20 µg/ml. After 60 min, Alpha Counts were read using an EnVision Plate Reader (Perkin-Elmer). Quadriplicates were performed in each experiment. Positive (ADRB2 receptor 125 nM / GST-GPRASP1-M 62.5 nM) and negative controls (only ADRB2 receptor 125 nM) were performed in 8 wells each. The Z' value was calculated according to the following formula (Zhang JH et al. 1999): Z'= 1 – [(3SD of sample + 3SD of control) / (mean of sample – mean of control). Data were analyzed in GraphPad Prism (version 4.0c), using nonlinear regression analysis for curve fitting.

3. Results

3.1 Identification of antibodies targeting the GASP motif

As an initial step, we analyzed the binding properties of the immune serum from a rabbit immunized against purified glutathione S-transferase fused to residues 924–1395 of GPRASP1 (previously described in Simonin et al., 2004). This carboxyl-terminal part (470 last residues) of GPRASP1, named in this study the original Antigen (o.Ag), contains the last three GASP motifs of GPRASP1 upstream to the entire C-ter domain that displays sequence homologies with the other members of the GPRASP/ARMCX protein family (Figure 1). We therefore analyzed potential cross reactivity of this serum with the closest homologues of GPRASP1 (GPRASP2, GPRASP3 and ARMCX5) in Western blot experiments. In addition, we used the GPRASP2-DM mutant protein (Bornert et al., 2013) in which the full consensus hydrophobic core SWFW present in two out of seven GASP motifs were substituted by four Alanine residues. Lysates of HEK293 cells overexpressing either GPRASP1, GPRASP2, GPRASP2-DM, GPRASP3 or ARMCX5 as fusion proteins with the Gaussia Luciferase C-ter domain (GLuc2, Table 1) were analyzed by immunoblotting analysis with the serum containing anti-GST-o.Ag antibodies. While analysis with anti-GLuc antibodies confirmed the overexpression of all fusion proteins (Figure 2 left panel), only overexpressed GLuc2-GPRASP1 and GLuc2-GPRASP2 were detected by anti-GST-o.Ag antibodies from the serum (Figure 2 right panel). The absence of detection of the mutant GPRASP2-DM, with mutated GASP motifs, as well as GPRASP3 and ARMCX5 suggests that the serum contains mainly antibody populations that detect GASP motifs present in GPRASP1 and GPRASP2. These results corroborate our previous observation showing that these anti-GST-o.Ag antibodies were able to detect the GPRASP1-Middle protein (i.e. the central part of GPRASP1 encompassing residues 380 to 1073; Figure 2) that contains 19 GASP motifs (Bornert et al., 2013) .

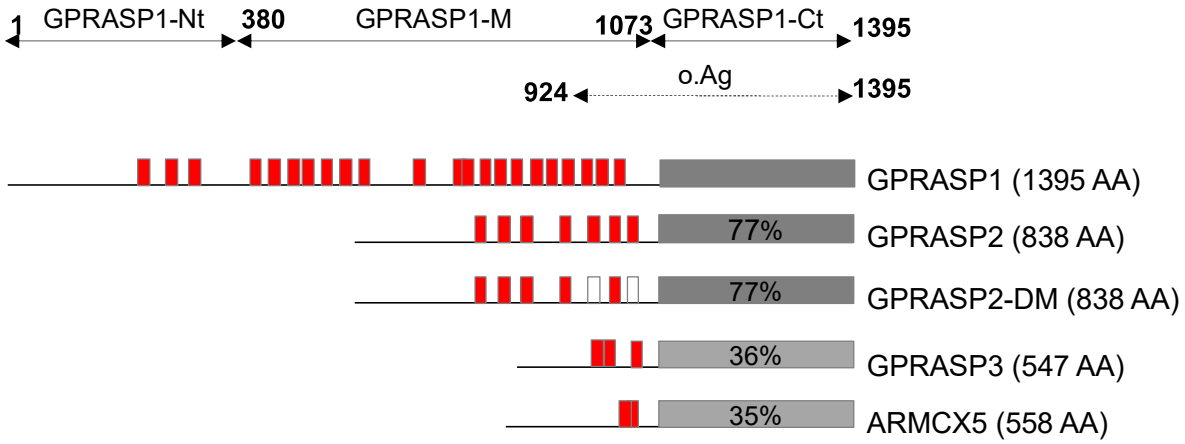

Figure 1. Schematic representation of four members of the GPRASP/ARMCX protein subfamily 1.

Grey boxes represent the conserved carboxyl-terminal domain of around 250 amino acids. The percent of identical amino acids shared with GPRASP1 is indicated within each box. Red boxes represent GASP motifs that correspond to the consensus sequence of 21 amino acids (GSEEEAIIG**SWFW**AEEEASME). Locations of GASP motifs are represented as a result of sequences analysis with the MEME SUITE web application 5.1.1 (Bailey et al., 2009; Kaeffer et al., 2021). The GPRASP2-DM double mutant protein (Bornert et al., 2013) is presented with the two GASP motifs (white boxes) out of seven in which SWFW kernels were substituted by AAAA residues. Polyclonal rabbit antibodies were raised against residues 924–1395 of GPRASP1 named the original GPRASP1 Antigen (o.Ag). The limits of the GPRASP1 amino-terminal (GPRASP1-Nt), central domain (GPRASP1-M) and carboxyl-terminal domains (GPRASP1-Ct) are indicated.

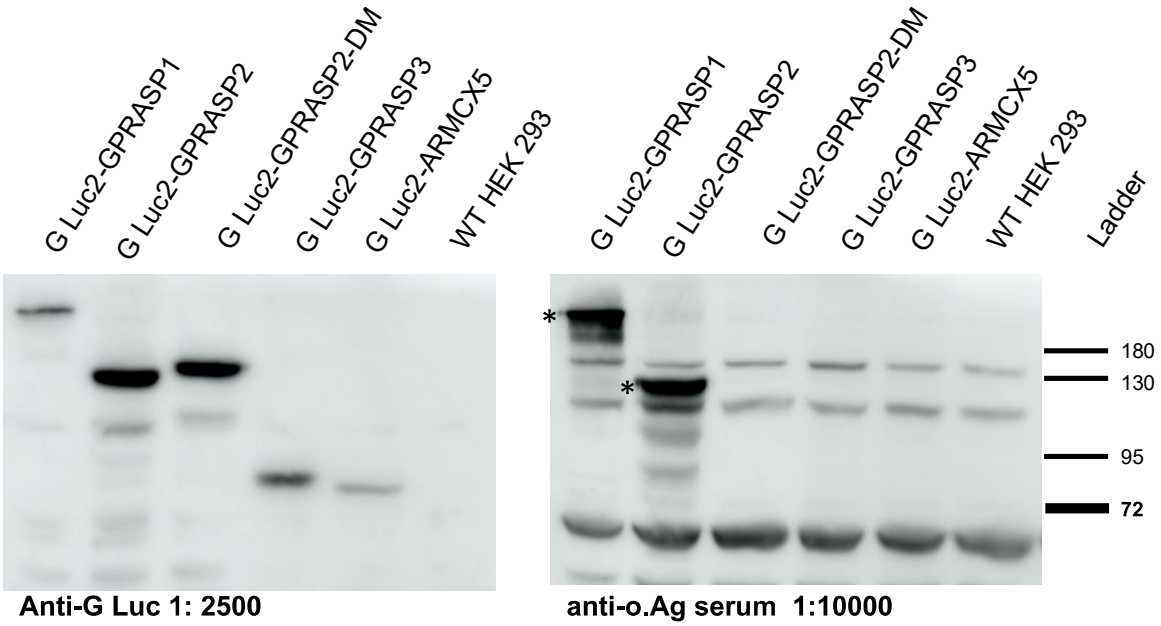

Figure 2 Identification of antibodies targeting GASP motifs.

Western Blot analysis of lysates of HEK293 cells overexpressing either GPRASP1, GPRASP2, GPRASP2-DM, GPRASP3 or ARMCX5 as fusion proteins with the C-ter of the *Gaussia princeps* luciferase GLuc2 fragment. The membranes were probed with anti-Gaussia luciferase antibodies (Anti-G Luc, left panel) or with the serum from rabbit inoculated with the original GST-GPRASP1 antigen (anti-o.Ag, right panel). Equivalent amounts of proteins (40 µg) were analyzed for each sample. The anti-o.Ag serum detected overexpressed G Luc2-GPRASP1 and G Luc2-GPRASP2 (protein bands tagged with asterisks) and reacted with at least 3 other proteins present in transfected and non-transfected HEK 293 cells extracts.

.

3.2 Characterization of affinity-purified antibodies subpopulations targeting GASP motifs by ELISA and Surface Plasmon Resonance (SPR)

To further characterize the recognition specificity of GPRASP1 polyclonal antibodies, we next decided to purify by affinity sub-populations of antibodies from the serum against GST-o.Ag. To this purpose, the IgG fraction from the immune rabbit serum was first isolated by conventional Protein G chromatography and the sub-populations of antibodies were then affinity-purified on sepharose-beads bound to MBP-o.Ag that contains the original GPRASP1 immunoreactive sequence, MBP-GPRASP1-Ct that contains no GASP motifs. MBP-GPRASP1-M that contains 19 out of the 22 GASP motifs but not the conserved GPRASP1 C-terminal domain and overlaps by approximately 150 amino acids with the o.Ag immunogen, including its 3 N-terminal GASP motifs. The 6xHis-GASP peptide encompasses only 3 GASP motifs (residues 800 to 889 of GPRASP1) that represent 70% of the amino acid sequence. Although these motifs are absent from the 3 GASP motifs present in o. Ag they display the highest homology to the GASP motif consensus sequence (Figure 3A). The three different GPRASP1 domains were produced and purified from *E. Coli* as MBP-fusion proteins while the GASP peptide was produced and purified from *E. Coli* as a 6xHis-fusion protein. The purified GPRASP1 domains were examined for purity by SDS-PAGE (Supplementary Figure S1) before coupling to Sepharose beads. The different GPRASP1 domains coupled to Sepharose beads were then used for affinity purification of the different subpopulations of antibodies from the polyclonal serum against GST-o.Ag. The final purified sub-populations of antibodies were assayed for protein concentration and examined for purity by Coomassie stained SDS-PAGE (Supplementary Figure S2). Approximately 0.25 mg of antibodies were purified per milliliter of serum. The subpopulation of antibodies affinity-purified from the MBP-o.Ag column was designated as “affinity-purified anti-o.Ag” (@ o.Ag) and represents antibodies against the entire immunogen except GST. The subpopulation of antibodies affinity-purified from the MBP-GPRASP1-M column was designated as “affinity-purified anti-GPRASP1-M” (@ GPRASP1-M). It represents antibodies against the central domain of GPRASP1 encoding 19 GASP motifs and corresponded to approximately 50% of the total affinity-purified anti-o.Ag antibodies. The subpopulation of antibodies affinity-purified from the MBP-GPRASP1-Ct column was designated as “affinity-purified anti-GPRASP1-Ct” (@ GPRASP1-Ct). It represents antibodies against the C-terminal sequence of GPRASP1 with no GASP motif and corresponded to

approximately 30% of the total affinity-purified anti-o.Ag antibodies. The subpopulation of antibodies affinity-purified on the 6xHis-GASP peptide column represented around 30% of the total affinity purified anti-o.Ag antibodies and was designated as “affinity-purified anti-GASP peptide” (@ GASP peptide).

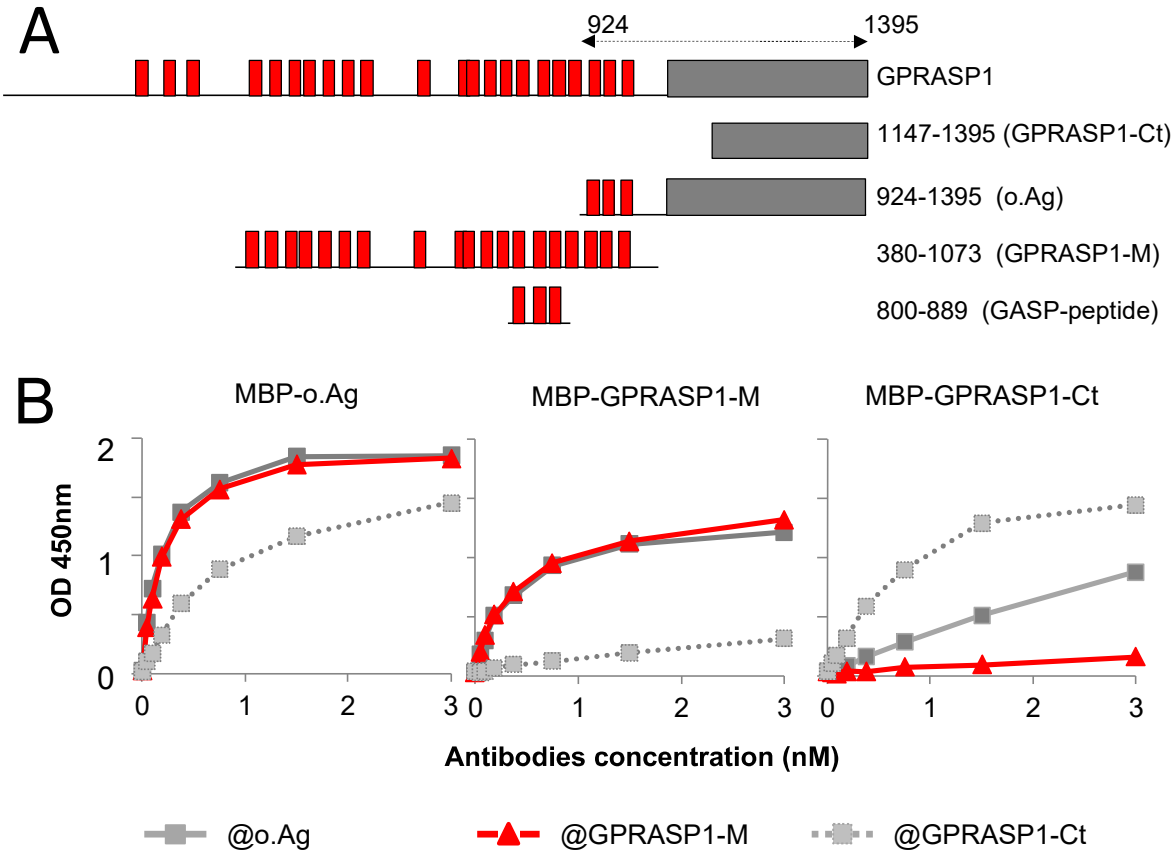

Figure 3. Two domains of GPRASP1 are recognized by antibodies from the serum raised against GST-o.Ag.

A. Scheme of GPRASP1 domains used for affinity purification of the seric antibodies raised against the original antigen fused to GST (GST-o.Ag). The antigens were all expressed as MBP-fusion proteins except for the GASP peptide that was fused to a 6xHis-tag.

B. Reactivity of each purified antibodies subpopulation in ELISA. Plates were coated with a fixed concentration of purified antigens, MBP-o.Ag (1 nM, left panel), MBP-GPRASP1-M (1 nM, middle panel) or MBP-GPRASP1-Ct (10 nM, right panel), and incubated with different concentrations of affinity-purified anti-o.Ag (@ o.Ag, dark grey squares), affinity purified anti-GPRASP1-M (@ GPRASP1-M, red triangles) and

affinity-purified anti-GPRASP1-Ct (@ GPRASP1-Ct, light grey squares). The optical density values (OD450nm) indicate the relative IgGs binding (for antibodies concentration ranging from 0.05 to 3 nM) to the coated antigens from a representative experiment (n = 2).

The binding abilities of affinity-purified antibodies sub-populations were subsequently assessed by enzyme-linked immunosorbent assays (ELISAs). We immobilized either MBP-o.Ag, MBP-GPRASP1-M or MBP-GPRASP1-Ct and incubated affinity-purified anti-GPRASP1 subpopulations of antibodies (o.Ag, GPRASP1-M and GPRASP1-Ct) at increasing concentrations (Seric antibodies showed no binding to MBP, Supplementary Figure S3A). As shown in Figure 3B, the binding curves confirmed the interaction of affinity-purified o.Ag antibodies with all three antigens (dark grey curves) and all three purified antibodies populations bind to the original antigen encoded in MBP-o.Ag (Figure 3B, left panel). As expected, the affinity-purified anti-GPRASP1-M antibodies did not bind to MBP-GPRASP1-Ct and, conversely, the affinity-purified anti-GPRASP1-Ct antibodies did not bind to the MBP-GPRASP1-M antigen (Figure 3B middle and right panels, respectively). These data fully confirmed the specificities of all three antibodies. Importantly, the affinity purified anti-GASP peptide antibodies showed similar binding reactivity than the affinity-purified anti-GPRASP1-M antibodies with the 6xHis-GASP peptide antigen in ELISA (Supplementary Figure S4B and S4C), indicating that these two antibodies subpopulations almost exclusively detect GASP motifs. This is not surprising since the GPRASP1-M domain, apart from the 19 GASP motifs shares less than 13% of its amino acid sequence (87/693) with the original GPRASP1 antigen (o.Ag).

Since in ELISAs the target antigens are adsorbed to hydrophobic solid surface which can lead to protein denaturation (Butler, 2000), we next assessed whether the affinity-purified o.Ag antibodies could bind to GST-GPRASP1, GST-GPRASP1-M and GST-GPRASP2-C fusion proteins captured through anti-GST antibodies in a hydrophilic matrix by Surface Plasmon Resonance (SPR) in order to quantitatively compare their binding capacities to the three different antigens. GPRASP2 is the closest GPRASP1 paralogue (Simonin et al., 2004) and GPRASP2-C displays 85 % sequence identity over the full sequence of the original antigen (471 aa), including 3 GASP motifs that display the highest sequence homology with the 3 GASP motifs present in the o.Ag. It should therefore have conserved the immunogenic epitopes that

are present in the o.Ag. Purified GST-fusion GPRASP1 full-length, GPRASP2-C and GPRASP1-M domains were immobilised on a sensor surface and the binding of two successive concentrations of affinity-purified anti-o.Ag antibodies to captured GST-fusions were compared. A GST-surface was used as the reference surface showing no binding since antibodies were affinity-purified on MBP-o.Ag columns (Supplementary Figure S4) and the raw binding profiles (Figure 4A) were normalized with respect to the molecular weight of each antigen by expressing the SPR antibodies responses in RU/ fmol.mm^{-2} (Figure 4B). Full-length GST-GPRASP1, GST-GPRASP2-C and GST-GPRASP1-M domains could significantly bind to o.Ag antibodies. Once normalized (Figure 4B), higher signals were observed for full-length GST-GPRASP1 and GST-GPRASP1-M as compared to GST-GPRASP2-C. This result suggests that GASP motifs may function as repeated epitopes allowing the binding of a higher number of antibodies on GST-GPRASP1 and GST-GPRASP1-M, which contains 22 and 19 GASP motifs, respectively, as compared to GST-GPRASP2-C that contains only 3 GASP motifs.

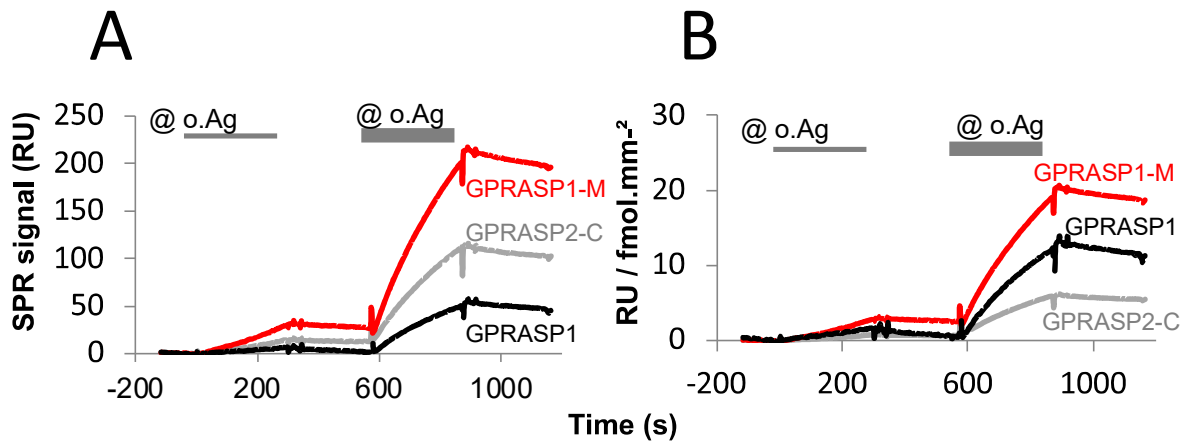

Figure 4 Comparison of SPR sensorgrams of anti-o.Ag antibodies binding to captured GPRASP antigens surfaces.

SPR experiments showing the binding of purified anti-o.Ag antibodies (@ o. Ag) to either captured GST-full-length GPRASP1 (700 RU ~4.1 fmol/mm²; bold black line), GST-GPRASP1-M (1160 RU ~10.5 fmol/mm²; red line) or GST-GPRASP2-C (1393 RU ~ 18.6 fmol/mm²; grey line). Two concentrations of purified anti-o.Ag antibodies were tested sequentially in one experiment (~10 and 100 µg/ml). SPR signals in relative unit were corrected for signals from the reference flow cell with GST alone (854

RU ~28,5 fmol/mm²; **(A)** then signals were normalized relative to target density as RU / fmol.mm² (**B**).

3.3 Validation of subpopulations of affinity-purified antibodies targeting GASP motifs by western blot, immunoprecipitation and immunofluorescence.

To evaluate the specificity of affinity-purified anti-o.Ag and anti-GASP-peptide antibodies subpopulations, we further performed immunoblotting of extracts from HEK293 cells overexpressing GLuc2-tagged GPRASP1, GPRASP2 and GPRASP2-DM. Since HEK293 cells display endogenous expression of GPRASP2 but no expression of GPRASP1, we also analyzed cell extracts from CRISPR/Cas9 generated GPRASP2 knock-out HEK293 cells in which a construct expressing full length GPRASP2 was transfected or not (Figure 4). As shown for the anti-o.Ag serum (Figure 2), purified anti-o.Ag and anti-GASP peptide antibodies detected overexpressed G Luc2-GPRASP1 and G Luc2-GPRASP2 but not G Luc2-GPRASP2-DM (Figure 5). The anti-o.Ag serum (Figure 2), the purified anti-o.Ag and anti-GASP peptide antibodies (figure 5) recognized a band with an apparent molecular weight of ~ 130 kDa in all HEK293 cell extracts. This band was absent in GPRASP2-KO HEK293 cell extracts but was present in cell extracts from GPRASP2-KO HEK293 transfected with the construct expressing full length GPRASP2, thus demonstrating that GPRASP2 is endogenously expressed in HEK293 cells and detected by the anti-GPRASP1 antibodies.

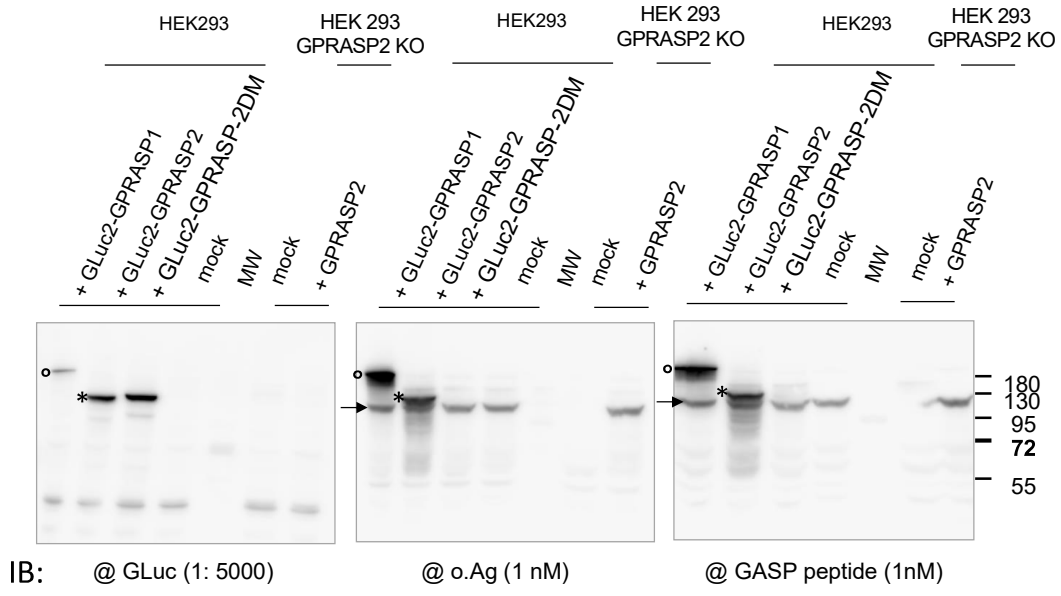

Figure 5. The purified anti-GASP motif antibodies detect GPRASP1 and GPRASP2 but not overexpressed G Luc2-GPRASP2-DM in western blot.
For each blot, lysates from HEK293 cells (4 left lanes) overexpressing a GLuc2 fusion protein with either GPRASP1, GPRASP2 or GPRASP2-DM, and lysates from GPRASP2-KO HEK293 cells (2 right lanes) overexpressing or not GPRASP2 were analyzed with the anti-Gaussia luciferase antibodies (@ GLuc; left) and the purified antibodies populations against o.Ag (@ o.Ag; middle) or the GASP peptide (@ GASP peptide; right) for immunoblotting (IB). The two anti-GPRASP1 antibodies recognized a ~ 195 kDa protein corresponding to GLuc2-GPRASP1 (labelled with °) and a ~130 kDa protein corresponding to GLuc2-GPRASP2 (labelled with *) as well as GPRASP2 (~120 kDa) which is endogenously expressed in HEK293 cells (arrow). MW (molecular weight ladder).

Results presented above indicates that both the 6xHis-GASP peptide and GPRASP1-M domain allowed to affinity-purify GASP1 motif specific antibodies. However, columns packed with the 6xHis-GASP peptide led to a lower antibody recovery than the ones packed with GPRASP1-M as compared to columns packed with the original antigen (30 and 50%, respectively). Moreover, we observed by ELISA that the flow-through of the 6xHis-GASP peptide column still contained antibodies that bind to GPRASP1-M, which was not the case when GPRASP1-M columns were used (data not shown). As these data indicated that GPRASP1-M was more efficient to purify anti-GASP motif antibodies we decided to further characterize anti-GPRASP1-M antibodies and to restrict the use of anti-GASP-peptide antibodies only in some critical experiments. We next evaluated whether overexpressed EYFP-GPRASP1 and YFP-GPRASP2 from CHO cell extracts could be immunoprecipitated with either affinity-purified anti-o.Ag or anti-GPRASP1-M antibodies and revealed in Western blot experiments with anti-GFP-HRP antibodies. It is noteworthy that we observed in previous experiments that CHO cells do not express endogenous GPRASP1 and GPRASP2 (not shown). As shown in Figure 6A, both antibodies efficiently immunoprecipitated full length GPRASP1 and GPRASP2 fused to YFP while no signal was observed in mock transfected CHO cells. We then performed immunofluorescence experiments with the same CHO cells overexpressing EYFP-GPRASP1 or YFP-GPRASP2 and anti-GPRASP1-M antibodies. As shown in Figure 6B, anti-GPRASP1-M antibodies could detect a specific signal (left panels) overlapping

with the YFP signal (middle panels) that was absent in WT CHO cells (lower panels), indicating that these antibodies specifically recognized GPRASP1 and GPRASP2 in a cellular context.

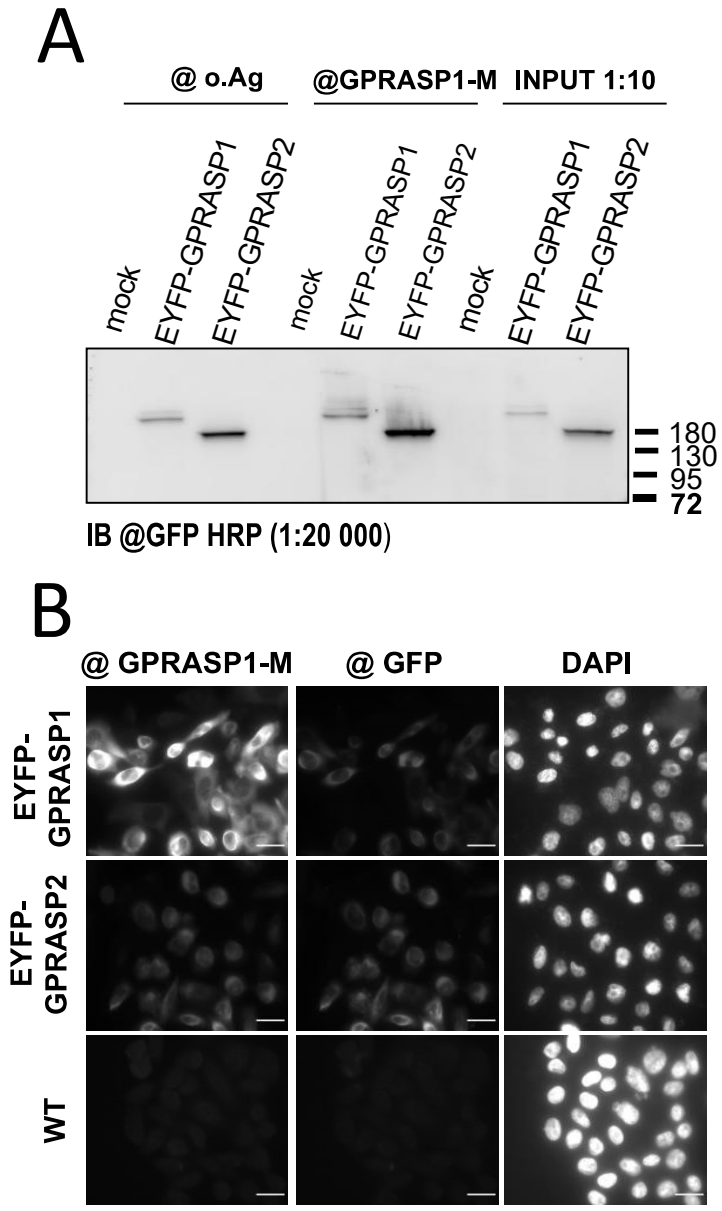

Figure 6. Purified anti-GASP motif antibodies detect GPRASP1 and GPRASP2 in immunoprecipitation and immunofluorescence studies.

A. Immunoblot of immunoprecipitates from CHO cells extracts stably expressing EYFP-GPRASP1 or EYFP-GPRASP2. Equivalent amounts of protein extracts (250 µg) were immunoprecipitated with affinity-purified anti-GPRASP1 antibodies populations 3 µg/mL for anti-o.Ag (@ o.Ag; left) and 0.45 µg/mL for anti-GPRASP1-M (@ GPRASP1-M; middle) and were separated by SDS-PAGE. EYFP-GPRASP1 or EYFP-GPRASP2 were revealed with an anti-GFP antibody (IB: @ GFP-HRP; 1: 20000).

B. Epifluorescence images of PFA-fixed CHO cells stably expressing EYFP-GPRASP1 or EYFP-GPRASP2 stained with affinity-purified antibodies against GPRASP1-M (@ GPRASP1-M, 1.5 µg/ml, left panel) or anti-GFP (@GFP, 0.5 µg/ml, middle panel) and with DAPI (right panel) Scale bar: 20 µm.

We further wanted to investigate whether affinity purified anti-o.Ag and anti-GPRASP1-M antibodies were able to selectively detect endogenous GPRASP1 and GPRASP2 expressed either in SH-SY5Y human neuroblastoma cells (Morales-Hernandez et al, 2020) or in mouse brain (Simonin et al, 2004). We therefore performed immunoblot experiments with SH-SY5Y cells and mouse brain extracts with both affinity-purified anti-o.Ag and anti-GPRASP1-M (Supplementary Figure S5). In Western blot experiments, both antibodies revealed two bands at the expected size of GPRASP1 (~ 195 KDa) and GPRASP2 (~ 120 KDa) in SH-SY5Y extracts and almost no background (Supplementary Figure S5). In brain extracts, anti-o.Ag and anti-GPRASP1-M antibodies revealed two major bands in western blot experiments corresponding to the expected size of GPRASP1 and GPRASP2 (Supplementary Figure S5). As expected, the upper band corresponding to GPRASP1 was absent in brain extracts of GPRASP1-KO mice (Boeuf et al., 2009) and the highest signal/noise ratio was observed with the anti-GPRASP1-M population of antibodies.

We also performed immunofluorescence assays with the same SH-SY5Y cells showing that anti-o.Ag and anti-GPRASP1-M antibodies mostly stained the cytoplasm (Supplementary Figure S6A, left upper and middle panels) and this signal was completely absent in the negative control with normal rabbit IgGs (Supplementary Figure S6A; left lower panels). Moreover, control immunofluorescence experiments with GPRASP2-KO HEK-293 cells, which do not show endogenous expression of GPRASP1, displayed only a low background signal (Supplementary Figure S6A right panels). Finally, we used HEK-293 cells stably expressing the GloSensor™ (HEK-293-Glo, Quillet et al., 2021), which display endogenous expression of both GPRASP1 and GPRASP2, to generate double KO for those two proteins and compared them to the same cells in which GPRASP1 was transiently reexpressed. Immunoblot and immunofluorescence experiments performed with those cell lines and anti-GPRASP1-M antibodies showed a high signal/noise ratio (supplementary Figures S6B and S6C, respectively). Together, these observations indicate that anti-GPRASP1-M antibodies can detect endogenous levels of GPRASP1 and GPRASP2.

3.4 Affinity-purified antibodies targeting GASP motifs inhibit ADRB2/GPRASP1-M interaction in a miniaturized AlphaScreen assay

In a previous study we have shown that the GASP motifs are essential for the interaction with C-tail of different GPCRs including β-adrenergic receptors ADRB1 and ADRB2, DOR, cannabinoid receptor type 2 CNR2 and muscarinic M1R (Bornert et al., 2013). Moreover, we have shown by SPR that the purified central domain of GPRASP1 (GST-GPRASP1-M) interacts with purified full-length solubilized ADRB2 (His-ADRB2) with an apparent affinity of 10 to 100 nM. On the basis of these data, we therefore decided to assess whether affinity purified anti-GPRASP1 antibodies could inhibit the interaction between purified ADRB2 and the central domain of GPRASP1. To this end, we setup a miniaturized assay based on the AlphaScreen technology that allows to use low amounts of purified material and provide sensitive and reproducible quantitative measurements. This bead-based, non-radioactive Amplified Luminescent Proximity Homogeneous Assay (AlphaScreen Assay) is adapted to test the capacities of the affinity-purified antibodies to compete for GST-GPRASP1-M binding with purified His-ADRB2 in a 384-well format. This no wash assay consists in the use of two types of nanobeads: the Glutathione donor beads loaded with a photosensitizer and the Nickel-chelate acceptor beads containing a chromophore. The proximity between beads, due to the interaction of the two proteins, is detected through the excitation of the donor bead with a laser at 680 nm, which leads to the production of a singlet oxygen, and the concomitant chemiluminescence in the acceptor bead upon exposure to singlet oxygen leading to the emission of light at 520-620 nm (Figure 7A). In a first step, the assay was adjusted with positive and negative controls of the interaction in order to obtain an optimal signal to noise ratio. The GST-GPRASP1-M and the His-ADRB2 concentrations were notably optimized using a cross titration experiment, using three concentrations for GST-GPRASP1-M (62.5 nM, 125 nM and 250 nM) and concentrations ranging from 125 to 2000 nM for His-ADRB2 (Supplementary Figure S7A). We then tested a larger range of ADRB2 concentrations (7.8 nM, 15.6 nM, 31.25 nM, 62.5 nM, 125 nM, 250 nM, 500 nM, 1000 nM and 2000 nM) with a fixed GST-GPRASP1-M concentration of 62.5 nM (Supplementary Figure S7B). A bell-shape response to His-ADRB2 increasing concentrations was observed with a maximum signal at 125 nM. This so-called “hook” effect frequently occurs in AlphaScreen assays since the excess of receptor inhibits the contact between the donor and acceptor

beads. We then tested the signal consistency of a positive control with a GST-His-tagged (10 and 30 nM) containing the two tags fused together with the donor and acceptor beads (Supplementary Figure S7C). A negative control was obtained with the same GST-His-tagged fusion protein to which either imidazole (200 nM) or glutathione (10 nM) was added. Another negative control in the assay was His-ADRB2 (125 nM) in the absence of GST-GPRASP1-M (Supplementary Figure S7D). Based on these experiments, the quality of the assay was measured by a statistical parameter – Z'– which takes into account the mean and standard deviation values for the positive and negative controls (Zhang et al., 1999). The calculated Z' and signal-to-background (S/B) corresponding to these control measurements were Z' > 0.72 with S/B > 58, confirming the robustness of the assay. Based on these controls, we chose the following conditions for further investigations: 62.5 nM GST-GPRASP1-M and 125 nM of His-ADRB2. We calculated the Z' and S/B for the ADRB2 receptor - GPRASP1-M interaction assay. Background signal was gauged either in the absence of GST-GPRASP1-M or with imidazole (200 nM) or glutathione (10 nM). The calculated Z' and S/B scores for these measurements were 0.6 and 8 (respectively) indicating satisfactory assay performance. Finally, Adenosine A2A receptor that poorly interacts with GPRASP1 in GST-pull down assay (not shown), produced no significant signal in this assay (Supplementary Figure S7E). In the conditions described above, increasing concentrations of affinity-purified anti-o.Ag antibodies, pre-incubated 1 h with GST-GPRASP1-M were able to compete for GST-GPRASP1-M binding to the His-ADRB2 with an IC50 of 116 ± 14nM (n=3) (Figure 7B). The purified anti-GASP-peptide antibodies showed similar inhibiting capacity (Supplementary Figure S8). These data show the potency of anti-GASP antibodies to inhibit the protein/protein interaction function of GASP motifs.

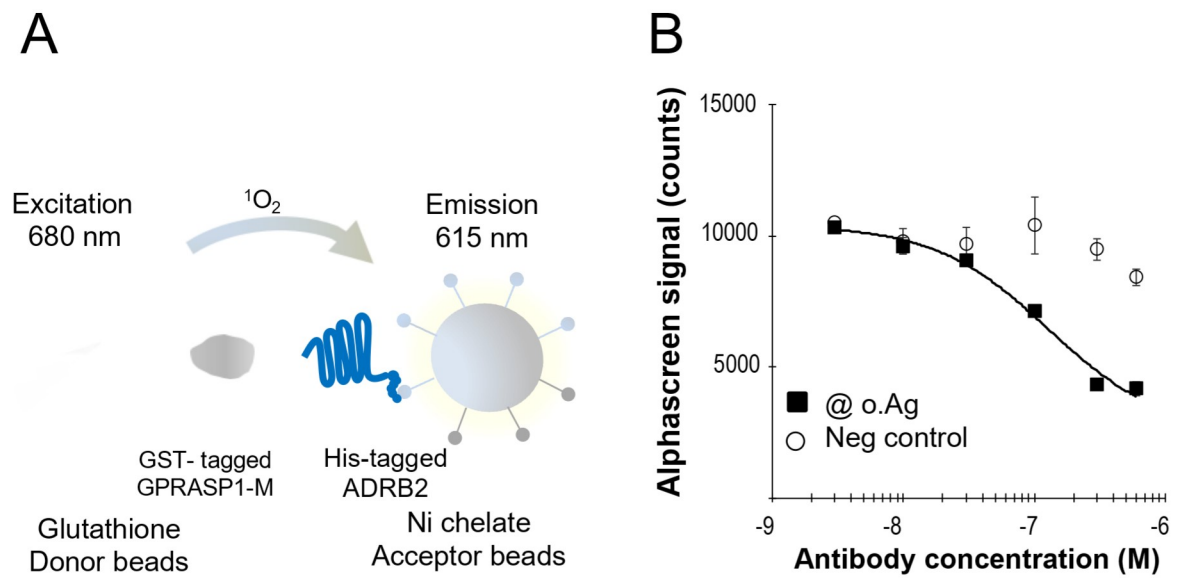

Figure 7. Purified anti-GPRASP1 antibodies inhibit ADRB2/GPRASP1-M interaction in a miniaturized AlphaScreen assay.

A. Scheme of the AlphaScreen interaction assay between His-tagged ADRB2 and GST-GPRASP1-M. If the donor and acceptor beads are in close proximity due to interaction between the two proteins, excitation of the donor beads at 680 nm results in the emission of light at 615 nm by acceptor beads. Glutathione-coated donor beads (for binding to GST-GPRASP1-M) and nickel chelate acceptor beads (for binding to His-tagged ADRB2 receptor) were used in this assay.

B. Competitive binding assay. The disruption of the association between ADRB2 and GPRASP1-M was evaluated by pre-incubation of the GST-GPRASP1-M with increasing amount of affinity-purified antibodies populations. The anti-o.Ag (@ o.Ag) inhibited the interaction between ADRB2 and GPRASP1-M proteins with an IC50 of 116 ± 14 nM whereas no competition was observed for the negative control (normal rabbit IgGs; Neg control; n=3).

4. Discussion

In the present study, we have characterized an anti-GPRASP1 serum obtained from a rabbit inoculated with a purified recombinant protein encoding the last 470 residues of human GPRASP1 fused to GST. This original antigen (o.Ag) includes 3 out of the 22 GASP motifs repeated in tandem in GPRASP1 and also the entire C-ter armadillo-like repeats domain of around 250 residues. We now show that around 50 % of the antibodies from this serum target GASP motifs instead of targeting the larger

conserved C-ter domain. This indicates that GASP motifs, which represent novel repeats unique to the GPRASP/ARMCX protein subfamily 1, display a good immunogenicity. Our previous data indicate that they may play a role in their protein-protein interactions (PPI) (Bornert et al., 2013; Kaeffer et al., 2021). In the present study, we describe the development of an AlphaScreen assay that allow to detect the interaction between purified ADRB2 and the central domain of GPRASP1 that contains most of the GASP motifs. In this assay, we show that purified antibodies that target GASP motifs efficiently block this interaction indicating that targeting GASP motifs could represent an interesting approach to inhibit the interaction between GPRASP1 and GPCRs.

Regarding the immunogenicity of the GASP motifs, we have proposed that the consensus sequence is GSEEEAIIGSWFWAEEEASME (Kaeffer et al., 2021). Intriguingly the central hydrophobic tetrapeptide SWFW is not considered to be immunogenic according to the Immune Epitope Database (IEDB) or the analysis resource Bepipred Linear Epitope Prediction 2.0 programs. Instead, it is the surrounding glutamate acidic residues on both sides of the SWFW sequence that score high for immunogenicity. Nevertheless, the SWFW sequences contribute to the detection of the protein target by the antibodies since GPRASP2-DM, in which the full consensus SWFW presents in two out of seven GASP motifs are substituted by alanine-tetrapeptides was detected neither by affinity-purified anti-o.Ag nor by affinity-purified anti-GASP motif antibodies using Western blot analysis. Our data also indicate that the antibodies purified and characterized in this study do not recognize all GASP motifs present in the different members of GPRASP subfamily 1 probably due to sequence variability of these different motifs. Indeed, the remaining five GASP motifs in human GPRASP2 contain the tetrapeptides MGSW, SSFW, FSFW, SWVL and SAYW as hydrophobic cores and not the complete consensus SWFW sequence (Kaeffer et al., 2021). In addition, GPRASP3 and ARMCX5, that contain GASP motifs, are detected neither by affinity-purified anti-o.Ag antibodies nor by affinity-purified anti-GASP motif antibodies using Western blot analysis. In ARMCX5, the two GASP motifs contain each the conserved SWFW sequences but the glutamate acidic residues in between are shared by the two tandem motifs: the 21 residues-long consensus sequences overlap. This is the reason why we have proposed that there are 1.5 GASP motifs in ARMCX5 instead of two (Kaeffer et al., 2021). Following this reasoning, GPRASP3 contains 2.5 GASP motifs: in Human, their central tetrapeptides are AWFW,

SWFW and NWFW, respectively. The only GASP motif with the fully conserved "SWFW" sequence is encoded in one of the two overlapping GASP motifs. It is probable as well that our antibodies bind tandem epitopes in a multivalent manner increasing their avidity and detect a unique GASP motif with low affinity. Our analysis by SPR also suggested that GASP motifs form repeated epitopes. Taken together, our data indicate that antibodies targeting GASP motifs need both the SWFW sequence together with acidic glutamate on both sides of the hydrophobic core to detect the antigen explaining why our antibodies detect neither GPRASP2-DM, GPRASP3 nor ARMCX5. ARMCX4, that also belongs to the GPRASP/ARMCX subfamily 1, was not included in our study since this large protein (2290 residues) displays very divergent GASP motifs (Kaeffer et al., 2021). As we have not tested ARMCX4 protein, we cannot completely rule out that our antibodies do not cross react with this protein. As was demonstrated for gene transcription (see Erlendsson and Teilum, 2021), one can speculate that avidity might participate in the regulation of the protein-protein interactions mediated by GASP motifs particularly for GPRASP1 and GPRASP2 that contains 22 and 7 GASP motifs, respectively. In the future, the role of avidity will have to be explored both in vitro and in cellular context.

In our present study, we set-up a quantitative miniaturized assay using the AlphaScreen method based on the interaction between the purified central domain of GPRASP1 and the purified G protein-coupled receptor ADRB2. Pre-incubation of the GPRASP1 central domain (62.5 nM) with increasing concentrations of affinity-purified anti-GASP motif antibodies could inhibit the interaction between this domain and the ADRB2 receptor (125 nM) with an IC50 of 115-145 nM. Although it was not possible to set-up this assay with the full length GPRASP1 due to difficulties to produce and purify this large protein (1395 aa) from bacteria, our results confirm that GASP motifs are necessary for mediating the interaction between the central domain of GPRASP1 and the entire receptor and that targeting these motifs with purified antibodies could allow the efficient neutralization of ADRB2-GPRASP1 interaction. They further suggest that the AlphaScreen assay described in this report might be useful for further screening of small molecule inhibitors of the interaction between GPRASP1 and the ADRB2 receptor. As GPRASP1 has been shown to be involved in adaptations associated with repeated stimulation of GPCRs like sensitization (Boeuf et al., 2009; Thompson et al., 2010) or tolerance (Tappe-Theodor et al., 2007) that are often considered as adverse side effects, antibodies or small molecules that block GPRASP1 interaction with

different GPCRs could represent an efficient way to limit adaptations associated with their chronic activation.

5. Conclusion

In this work we affinity-purified and characterized by Western blotting, immunofluorescence and SPR, anti-GPRASP1 polyclonal antibodies targeting a short repeated sequence called the GASP motif. We further set up a miniaturized AlphaScreen assay that allow to detect quantitatively the interaction between purified central domain of GPRASP1 and ADRB2. In the future, this assay will be useful to identify small molecules that block the interaction of GPRASP1 with GPCRs. In this AlphaScreen assay anti-GASP motif antibodies efficiently compete for the interaction between GPRASP1 central domain and ADRB2. Although this work makes the proof of concept that targeting GASP motifs with antibodies could represent an efficient way to block the interaction of GPRASP1 with GPCRs, the development of mono-specific tools such as monoclonal antibodies or nanobodies targeting a specific GASP motif to compete for the interaction of GPRASP1 with GPCRs will probably represent a more promising strategy both in terms of specificity and unlimited availability.

Acknowledgments.
We thank Dr. Jeremy Garwood for critical reading of the manuscript. We thank warmly all the actual and former members of the GPCRs pain and inflammation team as well as those from the IMPRESS platform for all the interdisciplinary scientific exchanges on the GPRASP projects. We are grateful to Marc Vigneron for helpful comments in CRISPR/Cas9 experimental design.

Author contributions.
Gabrielle Zeder-Lutz conceived and performed all the experiments but the AlphaScreen studies, and participated in writing the manuscript
Olivier Bornert set-up the purification of ADRB2, GST-GPRASP1-M, set-up the AlphaScreen assay
Rosine Fellmann-Clauss optimized the purification of ADRB2 and GST-GPRASP1-M, optimized the AlphaScreen assay.
Adeline Knittel-Obrecht performed the AlphaScreen assay.

Thibaud Tranchant, participated in the optimization of the AlphaScreen assay, generated the GPRASP2-KO HEK293 cells.
Sarah Bouteben participated in the purification of ADRB2 and GPRASP1-M.
Juliette Kaeffer dissected out brains of GPRASP1-KO mice.
Raphaëlle Quillet participated to experiments.
Pascal Villa supervised the AlphaScreen assay.
Renaud Wagner supervised protein expression and purification experiments.
Sandra Lecat conceived and participated to experiments, supervised the study and contributed to the writing of the manuscript.
Frédéric Simonin conceived the experiments, supervised the study and the writing of the manuscript.

Declarations of Interest.
none

Fundings.
This research was funded by the CNRS, Region Grand-Est, LABEX Medalis (ANR-10-LABX-0034, Programme d'investissement d'avenir), graduate school of pain EURIDOL of the University of Strasbourg (ANR- 17-EURE-0022, Programme d'investissement d'avenir), IdEx Unistra (ANR-10-IDEX-0002) and by the SFRI-STRAT'US project (ANR-20-SFRI-0012) under the framework of the French Program "Investments for the Future" given to the Strasbourg Drug Institute (IMS), as part of the Interdisciplinary Thematic Institute (ITI) 2021-2028 program of the University of Strasbourg, CNRS and Inserm.

References

Abu-Helo, A., and Simonin, F. (2010). Identification and biological significance of G protein-coupled receptor Associated Sorting Proteins (GASP). Pharmacology & therapeutics *126*, 244-250.

Bailey, T.L., Boden, M., Buske, F.A., Frith, M., Grant, C.E., Clementi, L., Ren, J., Li, W.W., and Noble, W.S. (2009). MEME SUITE: tools for motif discovery and searching. Nucleic acids research *37*, W202-W208.

Boeuf, J., Trigo, J.M., Moreau, P.H., Lecourtier, L., Vogel, E., Cassel, J.C., Mathis, C., Klosen, P., Maldonado, R., and Simonin, F. (2009). Attenuated behavioural responses to acute and chronic cocaine in GASP-1-deficient mice. The European journal of neuroscience *30*, 860-868.

Bornert, O., Moller, T.C., Boeuf, J., Candusso, M.P., Wagner, R., Martinez, K.L., and Simonin, F. (2013). Identification of a novel protein-protein interaction motif mediating interaction of GPCR-associated sorting proteins with G protein-coupled receptors. PloS one *8*, e56336.

Butler, J.E. (2000). Enzyme-linked immunosorbent assay. Journal of Immunoassay *21*, 165-209.

Erlendsson, S. and Teilum, K. (2021). Binding Revisited-Avidity in Cellular Function and Signaling. Frontiers in Molecular Biosciences 7, 615565.

Jung, B., Padula, D., Burtscher, I., Landerer, C., Lutter, D., Theis, F., Messias, A.C., Geerlof, A., Sattler, M., Kremmer, E.*, et al.* (2016). Pitchfork and Gprasp2 Target Smoothened to the Primary Cilium for Hedgehog Pathway Activation. PloS one *11*, e0149477.

Kaeffer, J., Zeder-Lutz, G., Simonin, F., and Lecat, S. (2021). GPRASP/ARMCX protein family: potential involvement in health and diseases revealed by their novel interacting partners. Current Topic in Medicinal Chemistry *21*, 227-254.

Kingston, R.E., Chen, C.A., and Okayama, H. (2003). Calcium phosphate transfection. In Current Protocols in Cell Biology.

Morales-Hernandez, A., Benaksas, C., Chabot, A., Caprio, C., Ferdous, M., Zhao, X., Kang, G., and MCKinney-Freeman, S. (2020). GPRASP proteins are critical negative regulators of hematopoietic stem cell transplantation. Blood *135*, 1111-1123.

Poirson, J., Biquand, E., Straub, M.L., Cassonnet, P., Nomine, Y., Jones, L., van der Werf, S., Trave, G., Zanier, K., Jacob, Y.*, et al.* (2017). Mapping the interactome of HPV E6 and E7 oncoproteins with the ubiquitin-proteasome system. The FEBS journal *284*, 3171-3201.

Quillet, R, Schneider, S, Utard, V, Drieu la Rochelle, A, Elhabazi, K, Henningsen, JB, Gizzi, P, Schmitt, M, Kugler, V, Simonneaux, V , Ilien, B, Simonin, F, Bihel, F. (2021). Identification of an N-acylated-DArg-Leu-NH2 Dipeptide as a Highly Selective Neuropeptide FF1 Receptor Antagonist That Potently Prevents Opioid-Induced Hyperalgesia. J.Med Chem *64*,7555-7564.

Simonin, F., Karcher, P., Boeuf, J.J., Matifas, A., and Kieffer, B.L. (2004). Identification of a novel family of G protein-coupled receptor associated sorting proteins. Journal of neurochemistry *89*, 766-775.

Stemmer, M., Thumberger, T., Del Sol Keyer, M., Wittbrodt, J., and Mateo, J.L. (2015). CCTop: An Intuitive, Flexible and Reliable CRISPR/Cas9 Target Prediction Tool. PloS one *10*, e0124633.

Stenberg, E., Persson, B., Roos, H., and Urbaniczky, C. (1991). quantitative-determination of surface concentration of proteins with surface-plasmon resonance using radiolabeled proteins. J Colloid Interface Sci *143*, 513-526.

Tappe-Theodor, A., Agarwal, N., Katona, I., Rubino, T., Martini, L., Swiercz, J., Mackie, K., Monyer, H., Parolaro, D., Whistler, J.*, et al.* (2007). A molecular basis of analgesic tolerance to cannabinoids. J Neurosci *27*, 4165-4177.

Thompson, D., Martini, L., Whistler, J.L. (2010). Altered ratio of D1 and D2 dopamine receptors in mouse striatum is associated with behavioral sensitization to cocaine. PLoS One *5*, e11038.

Vollmer, J.Y., Alix, P., Chollet, A., Takeda, K., Galzi, J.L. (1999). Subcellular compartmentalization of activation and desensitization of responses mediated by NK2 neurokinin receptors. J. Biol. Chem. *274*, 37915-37922.

Whistler, J.L., Enquist, J., Marley, A., Fong, J., Gladher, F., Tsuruda, P., Murray, S.R., and Von Zastrow, M. (2002). Modulation of postendocytic sorting of G protein-coupled receptors. Science (New York, NY) *297*, 615-620.

Zhang, J.H., Chung, T.D.Y., Oldenburg, K.R.A. (1999). A simple statistical parameter for use in evaluation and validation of high throughput screening assays. J. Biomol. Screen. *4*, 67–73

Table 1 Information on the different constructs used in this study

Name of the fusion protein	GPRASP/ARMCX domain or protein	GPRASP/ARMCX residues	Vector	Nter-tag or Nter-protein	Goal	Assays	Name of the antibodies subpopulations	References
MBP-o.Ag	o.Ag	924-1395	pMalC2	Maltose Binding protein	Production, purification in E.coli	Affinity columns for antibodies purification, ELISA	Affinity purified anti-o.Ag	This publication
MBP-GPRASP1-Ct	GPRASP1-Ct	1147-1395	pMalC2x				Affinity purified anti-GPRASP1-Ct	
MBP-GPRASP1-M	GPRASP1-M	380-1073	pMalC2x				Affinity purified anti-GPRASP1-M	
6xHis-GASP peptide	GASP motif	800-889	pET28b	Hexa-Histidine			Affinity purified anti-GASP-peptide	
GST-GPRASP1	GPRASP1	1-1395	pGEX-4T3	Glutathione S transferase	Production, purification in E.coli	SPR		This publication
GST-o.Ag	o.Ag	924-1395	pGEX-4T3			Rabbit immunization	Anti-GST-o.Ag serum	Simonin et al. 2004
GST-GPRASP2-C	GPRASP2-C	367-838	pGEX-4T3			SPR		This publication
GST-GPRASP1-M	GPRASP1-M	380-1073	pGEX-4T3			SPR, AlphaScreen		Bornert et al. 2013
GPRASP1	GPRASP1	1-1395	pcDNA3		Overexpression in mammalian cells	Western Blot (WB)		Simonin et al. 2004
GPRASP2	GPRASP2	1-838	pcDNA3					Bornert et al. 2013
GPRASP2-DM	GPRASP2-DM	1-838	pcDNA3					Bornert et al. 2013
GPRASP3	GPRASP3	1-547	pcDNA3.1					Bornert et al. 2013
ARMCX5	ARMCX5	1-558	pcDNA3.1					Bornert et al. 2013
GLuc2-GPRASP1	GPRASP1	1-1395	pSPICA-N2	Cter of Gaussia Luciferase	Overexpression in mammalian cells	Western Blot (WB)		Lecat et al. In preparation
GLuc2-GPRASP2	GPRASP2	1-838	pSPICA-N2					
GLuc2-GPRASP2-DM	GPRASP2-DM	1-838	pSPICA-N2					
GLuc2-GPRASP3	GPRASP3	1-547	pSPICA-N2					
GLuc2-ARMCX5	ARMCX5	1-558	pSPICA-N2					
EYFP-GPRASP1	GPRASP1	1-1395	pcDNA3.1	EYFP	Overexpression in mammalian cells	Immunofluorescence		This publication
EYFP-GPRASP2	GPRASP2	1-838	pcDNA3.1					

Supplementary Figures Captions

Figure S1. SDS Polyacrylamide gel analysis of affinity purified GPRASP1 protein domains stained by coomassie blue.

The preparations were enriched with GPRASP1 domains of interest (indicated with an asterisk*) and were used as antigens for seric antibodies purification. MW (molecular weight ladder).

Figure S2. SDS Polyacrylamide gel and Western blot analysis of affinity purified anti-GPRASP1 antibodies sub populations.

Gels were loaded with 2.5 µg of proteins (1.5 µg anti-GASP peptide antibodies) before staining. Gels for western blot analysis were loaded with 0.25 or 0.15 µg proteins and the IgG heavy chains were revealed with a goat anti-rabbit IgG secondary antibody (IRDye800 fluorophore or HRP for the blot with anti-GASP peptide antibodies). Purified anti-o.Ag, anti-GPRASP1-M, anti-GPRASP1-Ct and anti-GASP peptide antibodies are abbreviated as follows: @ o.Ag, @ GPRASP1-M, @ GPRASP1-Ct and @ GASP peptide. IgG- heavy chains and light chains (IgG-Hc and IgG-Lc, respectively) are indicated. MW (molecular weight ladder).

Figure S3 Characterization of anti-GPRASP1 antibodies sub populations by ELISA.

A. ELISA plates were coated either with MBP or MBP-o.Ag (concentration ranging from 62,5 to 500 ng / well). Both antigens were tested with the serum (dilution 5000x; left) and anti-MBP monoclonal antibody (dilution 5000x; Ig-MBP-AS Euromedex); right). **B.** Binding capacities of each purified antibodies subpopulation (1 nM) were tested by ELISA with plates coated either with no antigen (blank) or GPRASP1 antigens at 1 nM: MBP-o.Ag (black), MBP-GPRASP1-M (red); MBP-GPRASP1-Ct (light grey); 6xHis-GASP-peptide (striped red, right secondary Y axis). Error bars represent SD of two tests performed in triplicates for 6xHis-GASP-peptide. **C.** Antibodies ELISA signal dependency to the dose of the coated GASP- peptide antigen (SD for triplicates). Purified anti-o.Ag, anti-GPRASP1-M, anti-GPRASP1-Ct and anti-GASP peptide antibodies are abbreviated as follows: @ o.Ag, @ GPRASP1-M, @ GPRASP1-Ct and @ GASP peptide.

Figure S4 Control of the specificity of affinity purified anti-o.Ag antibodies

SPR experiments showing the binding of affinity purified anti-o.Ag antibodies (@ o.Ag) to either captured GST-fusion proteins full-length GPRASP1 (700RU ~4.1 fmol/mm², bold black line), GST-GPRASP1-M (1160 RU ~10.5 fmol/mm², red line) or GST-GPRASP2-C (1393 RU ~ 18.6 fmol/mm², grey line). Two concentrations of purified anti-o.Ag antibodies were tested sequentially in one experiment (~10 and 100µg/mL). SPR signals are shown in relative units (RU). As expected, the signals from the reference flow cell with GST alone (854 RU) returned to baseline (RU = 0) after injection of each antibody, showing no binding with GST, since the serum was affinity-purified on MBP-o.Ag columns.

Figure S5. Purified anti-GASP motif antibodies detect endogenously expressed GPRASP1 and GPRASP2 in Western blot studies.

Immunoblot analysis of lysates from SH-SY5Y cells (left; 50 µg of proteins) and mouse brain homogenates of WT (+/+) and GPRASP1-KO mice (right; 40 µg of proteins) with purified anti-o.Ag antibodies (@ o.Ag, 0.15 µg/ml) and anti-GPRASP1-M antibodies (@ GPRASP1-M, 0.8 µg/ml). The indicated primary antibodies recognized a ~195 kDa band corresponding to GPRASP1 and a ~ 120 kDa band corresponding to GPRASP2. Lower background signal was observed with purified anti-GPRASP1-M antibodies as compared to purified anti-o.Ag antibodies.

Figure S6. Immunofluorescence with affinity-purified anti-GASP motif antibodies allows detection of GPRASP1 and GPRASP2.

A. Confocal images of PFA- fixed SH-SY5Y cells (left) and GPRASP2-KO HEK293 cells (right) stained with DAPI (DNA) and purified anti-o.Ag antibodies population (@-o.Ag 1,5 µg/ml, upper panel) and anti-GPRASP1-M (@ GPRASP1-M, 1,5 µg/ml, middle panel)**.** Normal rabbit IgGs (3 µg/ml, lower panel) were used as negative control and show no labelling on both fixed SH-SY5Y cells and GPRASP2-KO HEK293 cells. Scale bar: 20 µm. **B.** Western blot analysis of crude extracts from HEK293-Glo cells with anti-o.Ag. Wild-type (WT) HEK293-Glo cells endogenously express both GPRASP1 and GPRASP2. A double GPRASP1-KO and GPRASP2-KO HEK293-Glo cell line generated by CRISPR-Cas9 (Zeder-Lutz G. unpublished data) was transiently transfected with empty (mock) or GPRASP1 (+GPRASP1) vector. Equivalent amounts of protein extracts (40 µg) were probed with affinity-purified anti-o.Ag antibodies (0.15

µg/ml). MW (molecular weight ladder). **C.** Epifluorescence images of PFA-fixed Double GPRASP1-KO and GPRASP2- KO HEK293-Glo cells transiently transfected with empty (mock) or GPRASP1 (+GPRASP1) plasmids were labelled with affinity-purified antibodies against GPRASP1-M (@ GPRASP1-M, 3.75 µg/ml, left panel) and with DAPI (right panel) Scale bar: 20 µm.

Figure S7. Optimization of the measurement conditions of the AlphaScreen test
A. Cross titration experiments. Interactions were measured for His-ADRB2 (concentrations ranging from 2000 to 125nM) and GST-GPRASP1-M (62.5 nM, 125 nM and 250 nM). The signal increases with increasing GST-GPRASP1-M concentrations and is maximal at saturation of glutathione donor beads (this is observed for GST-GPRASP1-M concentrations above 62.5 nM). The signal was inversely proportional to His-ADRB2 concentrations due to a saturation of Ni-chelate acceptor beads in presence of an excess of receptor (>125 nM) which inhibits association of both binding partners and causes a progressive signal decrease. **B**. Saturation curve showing a hooking effect. The signal increases with increasing concentrations of ADRB2, until reaching the hook point at 125 nM. At this point, the signal begins to decrease with increasing concentrations of ADRB2. **C and D.** Capture of donor and acceptor beads control experiments. Capture of a positive control consisting of a His-tagged GST (10 and 30 nM) was inhibited with either 200 mM imidazole or 10 mM glutathione (**C**). Similar signal inhibition was observed for the capture of both 62.5 nM His-ADRB2 and 125 nM GST-GPRASP1-M (D). **E**. Binding specificity of GST-GPRASP1-M - His-ADRB2 interaction. No interaction signal was observed when the adenosine AA2A receptor was tested instead of ADRB2.

Figure S8. Purified anti-GASP motif antibodies inhibit ADRB2/GPRASP1-M interaction in a miniaturized AlphaScreen assay.
The disruption of the association between ADRB2 and GPRASP1-M was evaluated by pre-incubation of the GST-GPRASP1-M with increasing amount of affinity-purified anti-GASP peptide antibodies (@ GASP peptide). These anti-GASP motif antibodies inhibit the interaction between ADRB2 and GPRASP1-M proteins with an IC50 similar to the one of the anti-o.Ag antibodies. Error bars represent SD of quadruplicates in one representative experiment.

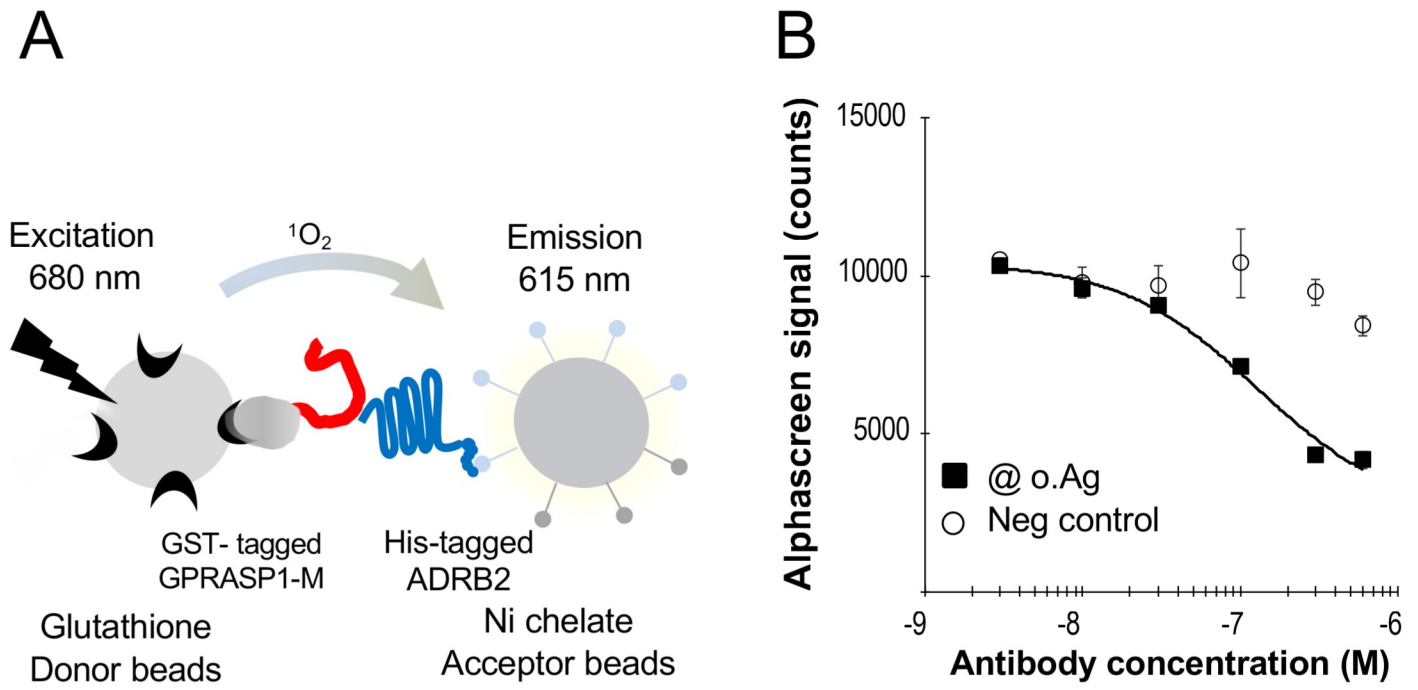

Figure 8

Author contributions.

Gabrielle Zeder-Lutz: Conceptualization, Methodology, Investigation, Writing - review & editing.

Olivier Bornert: Methodology, Investigation.

Rosine Fellmann-Clauss: Methodology, Investigation.

Adeline Knittel-Obrecht: Methodology, Investigation.

Thibaud Tranchant: Methodology, Investigation.

Sarah Bouteben: Methodology, Investigation.

Juliette Kaeffer: Methodology, Investigation.

Raphaëlle Quillet: Methodology, Investigation.

Pascal Villa: Supervision.

Renaud Wagner: Supervision.

Sandra Lecat: Supervision, Conceptualization, Methodology, Investigation, Writing - review & editing.

Frédéric Simonin: Supervision, Writing - review & editing.

Declaration of interest

The authors declare no conflict of interest